

Tetraiodothyroacetic Acid (Tetrac) and Nanoparticulate Tetrac Arrest Growth of Medullary Carcinoma of the Thyroid

M. Yalcin, E. Dyskin, L. Lansing, D. J. Bharali, S. S. Mousa, A. Bridoux, A. H. Herberg, H. Y. Lin, F. B. Davis, G. V. Glinsky, A. Glinskii, J. Ma, P. J. Davis, and S. A. Mousa

The Pharmaceutical Research Institute (M.Y., E.D., L.L., D.J.B., S.S.M., A.B., S.A.M.), Albany College of Pharmacy and Health Sciences, Albany, New York 12208; Uludag University (M.Y.), Veterinary Medicine Faculty, Department of Physiology, Gorukle, 16059 Bursa, Turkey; Cleveland Clinic (A.H.H.), Cleveland, Ohio 44195; and Signal Transduction Laboratory (H.Y.L., F.B.D., P.J.D.), and Functional and Translational Genomics (G.V.G., A.G., J.M.), Ordway Research Institute, Albany, New York 12208

Context: Tetraiodothyroacetic acid (tetrac) blocks angiogenic and tumor cell proliferation actions of thyroid hormone initiated at the cell surface hormone receptor on integrin $\alpha v \beta 3$. Tetrac also inhibits angiogenesis initiated by vascular endothelial growth factor and basic fibroblast growth factor.

Objective: We tested antiangiogenic and antiproliferative efficacy of tetrac and tetrac nanoparticles (tetrac NP) against human medullary thyroid carcinoma (h-MTC) implants in the chick chorioallantoic membrane (CAM) and h-MTC xenografts in the nude mouse.

Design: h-MTC cells were implanted in the CAM model ($n = 8$ per group); effects of tetrac and tetrac NP at $1 \mu\text{g}/\text{CAM}$ were determined on tumor angiogenesis and tumor growth after 8 d. h-MTC cells were also implanted sc in nude mice ($n = 6$ animals per group), and actions on established tumor growth of unmodified tetrac and tetrac NP ip were determined.

Results: In the CAM, tetrac and tetrac NP inhibited tumor growth and tumor-associated angiogenesis. In the nude mouse xenograft model, established $450\text{--}500 \text{ mm}^3$ h-MTC tumors were reduced in size over 21 d by both tetrac formulations to less than the initial cell mass (100 mm^3). Tumor tissue hemoglobin content of xenografts decreased by 66% over the course of administration of each drug. RNA microarray and quantitative real-time PCR of tumor cell mRNAs revealed that both tetrac formulations significantly induced antiangiogenic *thrombospondin 1* and apoptosis activator gene expression.

Conclusions: Acting via a cell surface receptor, tetrac and tetrac NP inhibit growth of h-MTC cells and associated angiogenesis in CAM and mouse xenograft models. (*J Clin Endocrinol Metab* 95:1972–1980, 2010)

A plasma membrane receptor for thyroid hormone has been identified on integrin $\alpha v \beta 3$ (1). The thyroid hormone signal at this cell surface receptor is transduced into an angiogenic response (2, 3) in endothelial cells and vascular smooth muscle cells that bear the receptor, as well as into a tumor cell proliferative response in cancer cells (4,

5). The proliferative response is generated by T_4 in physiological concentrations and by T_3 in concentrations that exceed physiological (1). The deaminated T_4 analog, tetraiodothyroacetic acid (tetrac), is an antagonist at the integrin receptor (1), rather than an agonist, and it blocks the binding of agonist thyroid hormone analogs to the integrin

ISSN Print 0021-972X ISSN Online 1945-7197
Printed in U.S.A.

Copyright © 2010 by The Endocrine Society

doi: 10.1210/jc.2009-1926 Received September 15, 2009. Accepted January 8, 2010.

First Published Online February 4, 2010

Abbreviations: bFGF, Basic fibroblast growth factor; CAM, chorioallantoic membrane; h-MTC, human MTC; MTC, medullary thyroid carcinoma; PLGA, poly(lactic-co-glycolic acid); Q-PCR, quantitative real-time PCR; tetrac, tetraiodothyroacetic acid; tetrac NP, tetrac nanoparticle; VEGF, vascular endothelial growth factor.

receptor. Within the cell, however, tetrac can have low potency thyromimetic activity (6). To limit the action of tetrac to the cell surface thyroid hormone receptor, we synthesized a tetrac nanoparticle (NP) that is excluded from the cell interior. The nanoparticle used in the studies reported here is tetrac bound at the outer ring hydroxyl by an ether linkage to poly(lactic-co-glycolic acid) (PLGA). The average length of the nanoparticle is 200 nm.

In addition to its inhibition of the cell surface effects on cell proliferation of thyroid hormone, tetrac is antiangiogenic in the absence of thyroid hormone (7). The thyroid hormone-tetrac receptor is located at the Arg-Gly-Asp (RGD) recognition site on integrin $\alpha v\beta 3$ (1, 8), which is important for interactions of the integrin with extracellular matrix proteins and growth factors (9). There is evidence for clustering of and crosstalk between the integrin and the vascular endothelial growth factor (VEGF) receptor (10) and basic fibroblast growth factor (bFGF) receptor (11). VEGF and bFGF are proangiogenic agents whose activity is blocked by RGD peptides and by tetrac (7).

In human breast cancer xenografts in the nude mouse, tetrac has been shown to inhibit tumor growth (12), presumably by its antiproliferative action. An antiangiogenic action in these studies was not explored. In the present studies, we examined the effects of unmodified tetrac and tetrac NP on the growth of xenografts of human medullary carcinoma of the thyroid gland and also estimated the vascularity of the treated tumors. RNA microarray analysis was also conducted on the cell line used in xenografts to identify changes in gene expression induced by tetrac formulations that may be relevant to angiogenesis. This tumor accounts for 8% of thyroid cancers and is a tumor that is poorly responsive to conventional chemotherapy (13). It occurs sporadically or may be a component of a genetically conditioned polyglandular tumor syndrome, multiple endocrine adenomatosis type 2 (14).

Materials and Methods

Materials

Polyvinyl alcohol, N-(3-dimethylaminopropyl)-N'-ethylcarbodiimide-hydrochloride, and the dialysis tubing cellulose membrane were purchased from Sigma Aldrich (St. Louis, MO). PLGA (70:30) was purchased from Polysciences Inc. (Warrington, PA). Ethylenediamine dihydrochloride was purchased from Pierce Biotechnology (Rockford, IL). Epoxy-tetrac intermediates were custom-synthesized by Azopharma Contract Pharmaceutical Services (Miramar, FL).

Obtained from Biocare Medical (Concord, CA) were Diva Pretreatment Solution (DV2004), aqua DePar (ADP1002), Mach 4 detection kit (M4U534), Background Sniper (BS966), rat antimouse CD31 detection kit (Predilute, RT517), Factor VIII (CP039, used at 1:100), wash buffer (TWB945), and DAB

(BDB 2004). Hemoglobin standard, Drabkin's reagent, and other common reagents were purchased from Sigma Aldrich.

PLGA nanoparticle

Nanoparticles were synthesized by modification of a method (single emulsion solvent diffusion) originally described by Jeffery *et al.* (15) and Song *et al.* (16). Amino-functionalized PLGA nanoparticles were obtained by conjugating these PLGA nanoparticles with ethylenediamine, using carbodiimide chemistry. Finally, amino-functionalized PLGA nanoparticles were reacted with tetrac intermediate, supplied by Azopharma Contract Pharmaceutical Services to obtain the final product, tetrac-conjugated PLGA nanoparticles. The custom-made intermediate of tetrac was composed of tetrac conjugated to epibromohydrin through the phenolic hydroxyl group present on it. This epoxy group reacts with the amino group (17, 18) present in the modified PLGA nanoparticles in aqueous condition. In a typical experiment, PLGA nanoparticles were synthesized by adding 200 μ l of PLGA (40 mg/ml in dimethylsulfoxide) to 20 ml of a 1% aqueous solution of polyvinyl alcohol. This mixture was constantly stirred for about 12 h at room temperature to form the nanoparticles. The nanoparticle suspension was then dialyzed for 6 h (membrane cutoff, 10–12 kD) to remove the impurities as well as the organic solvent. To 18 ml of this void PLGA nanoparticulate solution were added 2 ml of PBS buffer (10X) and 500 μ l of N-(3 dimethylaminopropyl)-N'-ethylcarbodiimide hydrochloride (180 mg/ml in 10X PBS). The mixture was magnetically stirred for about 1 h, followed by another addition of 500 μ l of ethylenediamine (280 mg/ml in 10X PBS), and stirring continued for at least 24 h. The whole solution was then dialyzed (10–12 kD cutoff membrane) for 10–12 h to eliminate unreacted materials. A stock solution of the custom-made epoxy-activated tetrac (Azopharma) in anhydrous dimethylsulfoxide (5 mg/ml) was prepared, and 100 μ l of this activated tetrac solution was added to 10 ml of the above amino-functionalized PLGA nanoparticles and stirred for at least 24 h. The solution was then dialyzed for at least 12 h for purification (12 kD cutoff membrane) and lyophilized. These lyophilized tetrac-conjugated PLGA nanoparticles were reconstituted in deionized water/PBS and used for the experiments described below.

Cells and cell culture

Human medullary thyroid carcinoma (h-MTC) cells (catalog no. CRL-1803) were purchased from the American Type Culture Collection (Manassas, VA) and cultured as instructed by the supplier, using a complete growth medium consisting of F-12K with 10% fetal bovine serum. Cells were cultured in 5% CO₂/air atmosphere at 37 C to subconfluence and then treated with 0.25% (wt/vol) trypsin/EDTA to effect cell release from the culture vessel. After washing with culture medium, the cells were suspended in DMEM that was free of phenol red and fetal bovine serum and were counted.

Tetrac vs. tetrac NP distribution in h-MTC cells

Cells were grown in F-12K medium (Invitrogen, Grand Island, NY) supplemented with 10% fetal calf serum (Atlanta Biologicals, Lawrenceville, GA). Penicillin and streptomycin (1%) were present in culture media. The cells were trypsinized and centrifuged, and the cell pellet was resuspended in the corresponding media. Then, 500 μ l of the suspension (~50,000 cells) were transferred to each well of a four-well glass slide (Chamber

Slide System; Nalge Nunc International, Naperville, IL) and incubated for 24 h at 37 C with 5% CO₂/95% air. The cells were treated with 20 μ l of unmodified tetrac tagged with Cy3 dye or with PLGA-tetrac tagged with Cy3 and separately incubated (37 C; 5% CO₂/95% air) for 2 h. After incubation, the plates were washed several times with PBS, then fixed in 1% formaldehyde (Sigma Aldrich), and treated with Vectashield (Vector Laboratories Inc., Burlingame, CA). Confocal images were obtained with a Leica TCS SP5 confocal microscope (Leica Microsystems, Wetzlar, Germany), using a 63X (NA = 1.3 glycerol immersion) objective. A 405-nm laser was used for excitation, and emission was detected between 565 and 688 nm.

Tumor growth in the chick chorioallantoic membrane (CAM) cancer implant model

The effects of tetrac and tetrac NP at 1.0 μ g/CAM on tumor angiogenesis and tumor growth (weight in milligrams) of 1×10^6 MTC cells implanted in Matrigel on 7-d-old CAMs were determined after a subsequent 8 d of implantation (19). Hemoglobin content of tumor masses was determined with Drabkin's reagent, as described in *Estimation of tumor response to tetrac or tetrac NP*. Data represent mean tumor weight (mg) and tumor hemoglobin (mg/dl) \pm SEM per treatment group (n = 8 per group).

Cell implantation in nude mice

Female NCr nude homozygous mice aged 5–6 wk with body weight of 20 g were purchased from Taconic Farms (Hudson, NY). Animals were maintained under specific pathogen-free conditions and housed four per cage under controlled conditions of temperature (20–24 C) and humidity (60–70%), with a 12-h light, 12-h dark cycle. Water and food were provided *ad libitum*. Mice were allowed to acclimate for 5 d before the start of treatments. Xenograft experiments were carried out in the animal research facility of the Veterans Affairs (VA) Medical Center, Albany, New York, and the experimental protocol was approved by the VA Institutional Animal Care and Use Committee.

Matrigel (BD Bioscience, San Jose, CA) was thawed overnight at 4 C and placed on ice. The tumor cells in exponential growth phase were harvested using 0.25% trypsin-EDTA, washed, and suspended in medium. Only suspensions of single cells with a viability exceeding 95% were used. Approximately 2×10^6 cells in 100 μ l of medium mixed with the same volume (100 μ l) of Matrigel were injected sc into the left and right flank regions of each mouse.

Treatment of animals with unmodified tetrac or tetrac NP

Tumors were measured daily by calipers, and tumor volume was calculated according to a standard formula ($W \times L^2/2$), where W = width and L = length. Tumor volume measurements were made every other day after the implant for the first 5 wk after inoculation, and tumor volumes were measurable by 33 d after implant, after which treatment was started. Mice with tumors of 225–275 mm³ in volume proximal to the injection site were randomized into three groups (n = 6): control group, tetrac (10 mg/kg) group, and tetrac NP (1 mg/kg) group. Drugs were administered ip daily for 21 d. Mice were weighed daily and tumor size was measured daily, starting on d 1 and continuing to the end of the experiment.

Estimation of tumor hemoglobin response to tetrac or tetrac NP

At the conclusion of the experiments, all animals were killed in a CO₂ chamber, and tumor masses were collected and weighed. Tumor mass hemoglobin content was measured to index vascularity of the tumor. For this purpose, each tumor mass was placed into a 0.5-ml tube of double-distilled H₂O and homogenized for 5–10 min. The samples were then centrifuged at 4000 rpm for 10 min, and the supernatants were collected for hemoglobin measurement. Fifty microliters of supernatant were mixed with 50 μ l Drabkin's reagent and allowed to sit at room temperature for 15–30 min; 100 μ l of this mixture was then placed in a 96-well plate, and absorbance was measured at 540 nm with a Microplate Manager ELISA reader (BioRad Laboratories, Hercules, CA). Hemoglobin concentration was determined by comparison with a standard curve in milligrams per milliliter.

Statistical analysis for CAM and xenograft studies

Statistical analysis was performed by one-way ANOVA, using Statview software (Adept Scientific, Acton, MA) and comparing the mean \pm SD from each experimental group with its respective control group. Statistical significance was defined as $P < 0.05$.

RNA microarray analysis

Extraction of RNA from h-MTC cells was by the method of Glinsky *et al.* (20, 21). Technical aspects of microarray studies, stringent quality control of microarray studies, and statistical analysis of gene expression were as described in our previous work (20–23). In brief, the array hybridization and processing, data retrieval, and analysis were carried out with standard sets of Affymetrix (Santa Clara, CA) equipment, software, and protocols in an Affymetrix microarray core facility. RNA was extracted from cell cultures of two independent biological replicates of each experimental condition and analyzed for sample purity and integrity using BioAnalyzer instrumentation (Agilent, Santa Clara, CA). Expression analysis of 54,675 transcripts was conducted for each sample, using Affymetrix HG-U133A Plus 2.0 arrays. Data retrieval and analysis were by MAS5.0 software (Affymetrix, Santa Clara, CA). Concordant changes of gene ex-

TABLE 1. Genetic targets analyzed using the Q-PCR method

Gene name	Gene symbol	TaqMan assay ID
Thrombospondin 1	THBS1	Hs00962914 m1
Vascular endothelial growth factor A	VEGFA	Hs00900058 m1
Fas (TNFRSF6)-associated factor 1	FAF1	Hs00165806 m1
Catenin (cadherin-associated protein), α 1	CTNNA1	Hs00944792 m1
Glyceraldehyde-3-phosphate dehydrogenase	GAPDH	Hs99999905 m1
DNA fragmentation factor, 45 Da, α polypeptide	DFFA	Hs01042658 g1
Caspase 8-associated protein 2	CASP8AP2	Hs01594273
Caspase 2	CASP2	Hs00892482 g1

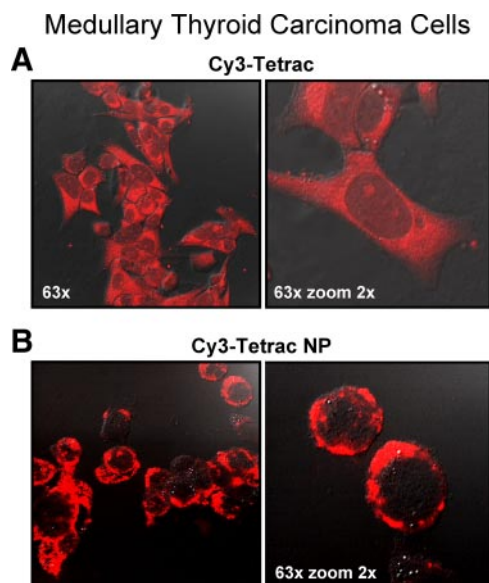


FIG. 1. Representative confocal images illustrating differences in the distribution in h-MTC cells of unmodified tetrac and tetrac NP. Cy3-labeled tetrac is homogeneously distributed in cytoplasm and over the nucleus (A). The distribution of Cy3-labeled tetrac NP (B) in this single view is nonhomogeneous; this reflects restriction of the molecule to the cell surface, confirmed on serial vertical images (data not shown).

pression for each experimental condition were determined at the statistical threshold P value < 0.01 (two-tailed t test).

Quantitative real-time PCR (Q-PCR) analysis of gene expression

That drug-induced changes in specific mRNA abundance observed in microarray experiments reflected gene expression was validated by Q-PCR. The latter was carried out with an ABI 7900HT real-time PCR System and TaqMan gene expression assays (Applied Biosystems, Foster City, CA) specifically designed for quantitative analysis of mRNA expression of the human genes listed in Table 1. As described above for the microarray analysis, RNA was extracted from cell cultures of two

independent biological replicates of each experimental condition and analyzed for sample purity and integrity using the BioAnalyzer instrumentation. Q-PCR assays for each gene were carried out in triplicate using *GAPDH* as a normalization control. The SDS 2.2 software platform was used for the computer interface with the ABI 7900HT PCR System (Software Diversified Services, Spring Lake Park, MN) to generate normalized data, compare samples, and calculate the relative quantity. Statistical significance of the difference in gene expression was estimated using the two-tailed t test.

Results

Tetrac vs. tetrac NP distribution within h-MTC cells

Confocal imaging revealed that unmodified tetrac was distributed throughout the MTC cell, whereas tetrac NP was restricted to the plasma membrane (Fig. 1).

Effect of tetrac and tetrac NP on tumor angiogenesis and tumor growth in the CAM model

MTC cells were implanted in 1×10^6 aliquots in the CAM model (7-d-old chick eggs; $n = 8$ eggs per group), and the effect of tetrac and tetrac NP at $1 \mu\text{g}/\text{CAM}$ was determined on tumor-related angiogenesis and tumor growth after implantation. Exposure of cells to either tetrac or tetrac NP resulted in effective inhibition ($P < 0.01$) of tumor growth (Fig. 2A). Tetrac and tetrac NP treatment resulted in significant inhibition ($P < 0.01$) of tumor-mediated angiogenesis (mg hemoglobin/ml) (Fig. 2B).

Response of human tumor xenografts to tetrac administration

Daily treatment of xenografted animals with tetrac (10 mg/kg ip) or tetrac NP (1 mg/kg ip) resulted in diminution in tumor volume by d 2 (Fig. 3, A and B), and

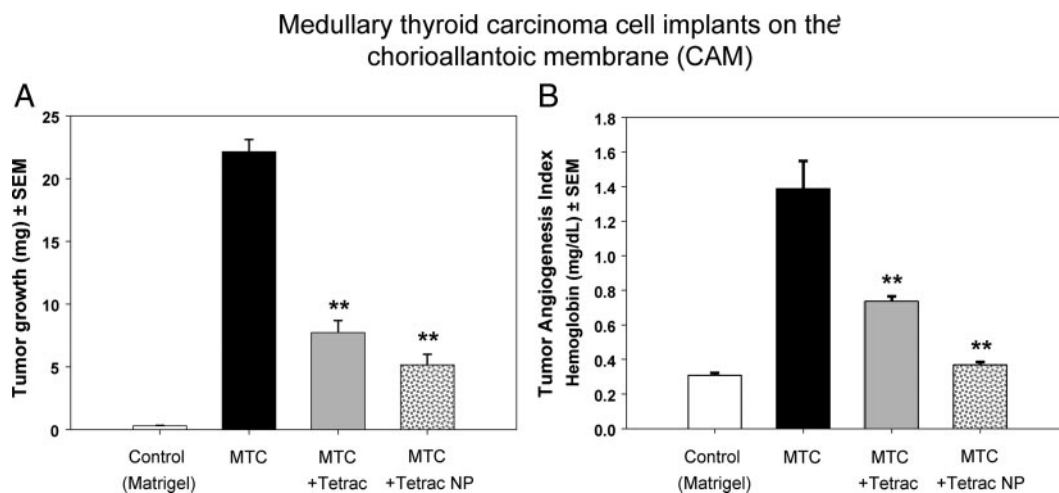


FIG. 2. The effect of tetrac and tetrac NP on human medullary carcinoma tumor growth (A) and tumor angiogenesis (B) in the chick CAM cancer cell implant model. Tetrac and tetrac NP were added at $1 \mu\text{g}/\text{CAM}$. Significant reductions in tumor size with both agents are evident. **, $P < 0.001$.

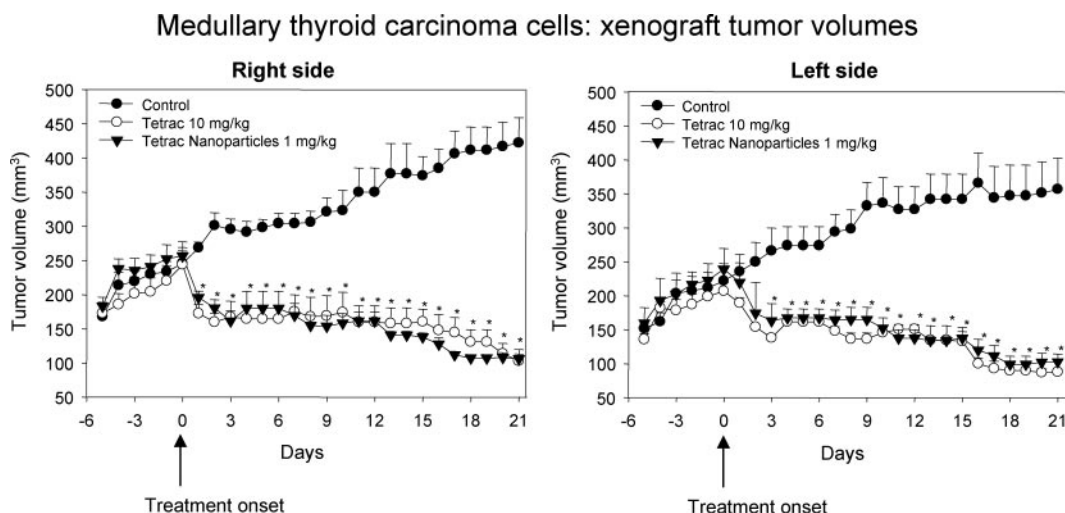


FIG. 3. The action of systemic tetrac and tetrac NP treatment on h-MTC flank xenograft volume in the nude mouse, compared with tumor volumes in untreated control animals. Data are expressed as mean tumor volume (mm³) ± SD; n = 6 animals per group. Right and left flank implants demonstrate consistency of tumor response. *, P < 0.01, either treatment group vs. control.

suppression of growth was sustained with administration of the formulations of tetrac for up to 21 d (Fig. 3, A and B) (P < 0.01).

At the end of the study, tumor weight was directly measured in the untreated, tetrac-treated, and tetrac NP-treated groups. Treatment with both tetrac (10 mg/kg ip) and tetrac NP (1 mg/kg ip) resulted in 65–80% reduction of tumor mass compared with controls (P < 0.01) (Fig. 4).

Effect of tetrac on an index of xenograft angiogenesis

Treatment with either tetrac (10 mg/kg ip) or tetrac NP (1 mg/kg ip) daily for 21 d resulted in reduction of 70–80% in tumor-associated neovascularization (P < 0.01), as evidenced by the hemoglobin levels in tumor tissue (Fig. 5).

Effect of tetrac on body weight

Daily treatment with tetrac (10 mg/kg ip) or tetrac NP (1 mg/kg ip) for 21 d did not result in a significant effect on incremental body weight growth in these groups, compared with the untreated group (data not shown).

mRNA analyses of h-MTC cells treated with tetrac or tetrac NP

Because tetrac NP does not gain access to the cell interior, the highly concordant effects of tetrac and tetrac NP on gene expression indicate that both formulations of tetrac express their effects via the cell surface receptor (1). Exposure of h-MTC cells to tetrac and to tetrac NP for 24 h resulted on microarray in significantly decreased abundance of mRNA of VEGFA, whose gene product is a potent angiogenesis activator, and a concomitant increase in the mRNA of the angiogenesis inhibitor protein, throm-

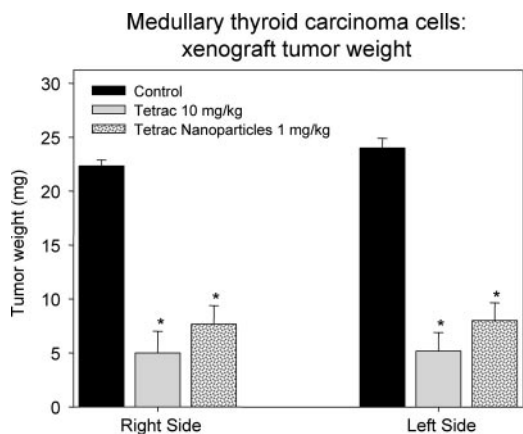


FIG. 4. The effect of tetrac and tetrac NP treatment on xenograft mass at time when animals were killed, compared with xenografts from untreated control animals. Data are expressed as mean tumor mass (mg) ± SD; n = 6 animals per group. *, P < 0.01, either treatment group vs. control.

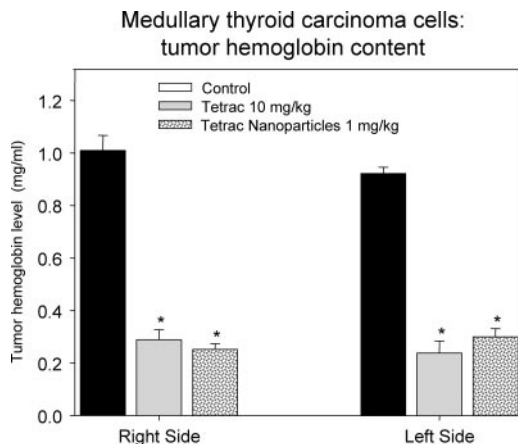


FIG. 5. The action of tetrac and tetrac NP on the h-MTC tumor mass hemoglobin levels, compared with control xenograft hemoglobin content. Data are expressed as mean hemoglobin levels (mg/ml) ± SD; n = 6 animals per group. *, P < 0.01, treatment group vs. control.

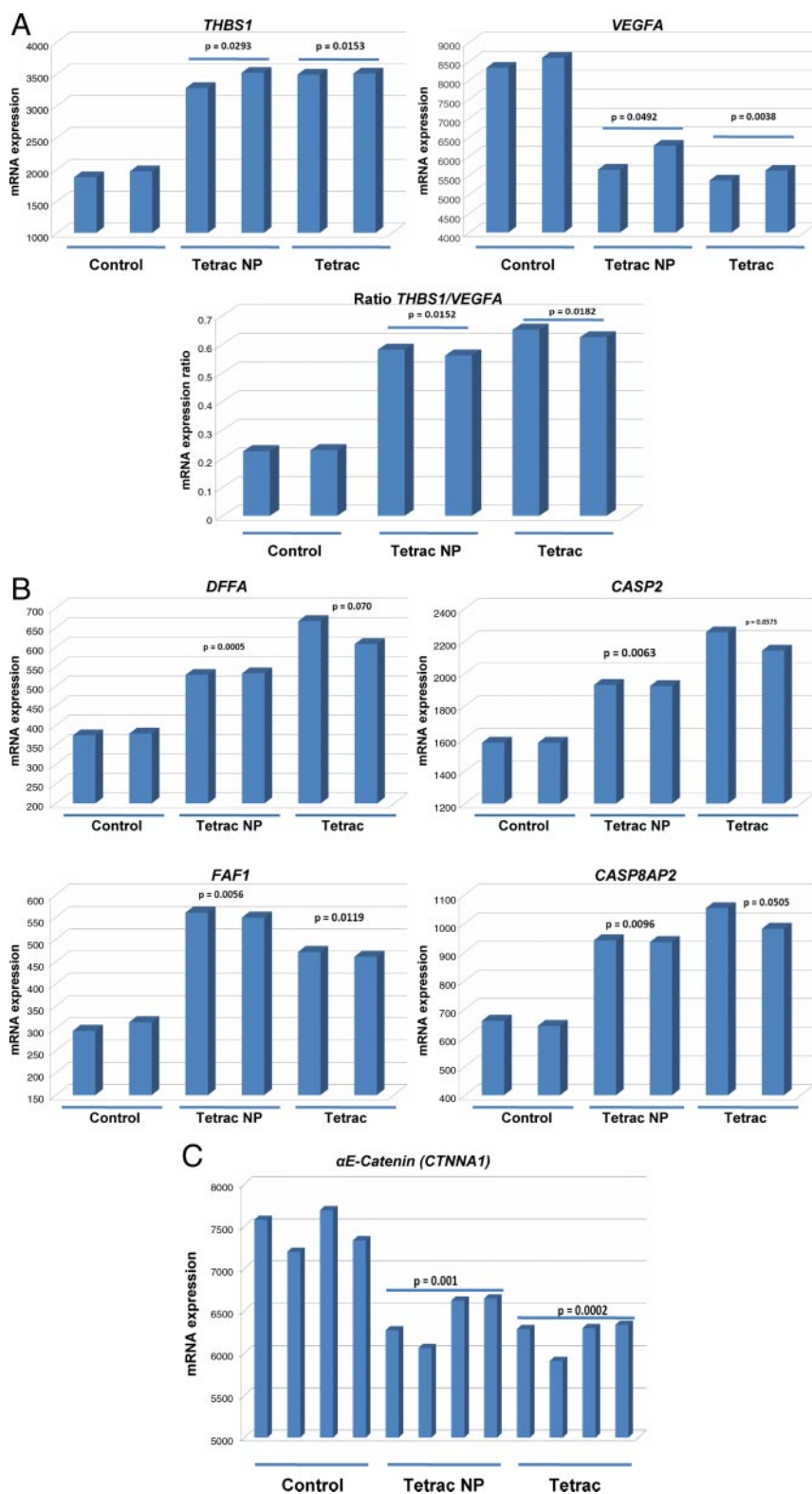


FIG. 6. RNA microarray results from h-MTC (TT) cells treated *in vitro* with tetrac or tetrac NP. A, Duplicate analyses of abundance on microarray of mRNAs of angiogenesis-relevant *THBS1* (*thrombospondin1*) and *VEGFA* genes in control and treated tumor cells and plotting of the ratio *VEGFA/THBS1*. B, Duplicate analyses of mRNAs of apoptosis-relevant *DFFA*, *CASP2*, *FAF1*, and *CASP8AP2* genes in control and treated tumor cells. C, Quadruplicate quantitation of abundance of the αE -catenin (*CTNNA1*) mRNA in control and treated h-MTC cells. The bars represent mean values, and *P* values were estimated using the two-tailed *t* test.

bospondin 1 (*THBS1*) (Fig. 6A). The mRNA expression ratio for *THBS1/VEGFA* was comparable for both formulations. This combination of findings provides a molecular basis for a strong antiangiogenic effect of tetrac and tetrac NP in the h-MTC xenograft model.

Tetrac NP also caused significant increases in abundance of mRNAs of genes associated with induction of apoptosis (Fig. 6B), including *caspase-2* (*CASP2*), *DFFA*, *FAF1*, and *CASP8AP2*. *CASP2* may be proapoptotic or function as a tumor suppressor (24). Unmodified tetrac significantly increased mRNAs of *FAF1* and *CASP8AP2*; increases in mRNAs of *DFFA* and *CASP2* by unmodified tetrac approached statistical significance. These microarray observations suggest that tetrac formulations have proapoptotic activity (12) beyond inhibition at the integrin receptor of the antiapoptotic actions we have described for agonist thyroid hormone analogs (5, 25).

Figure 6C shows that mRNA abundance of αE -catenin (*CTNNA1*) is decreased in h-MTC cells by both tetrac and tetrac NP. The roles of *CTNNA1* protein in cancer cells are complex, but *CTNNA1* may support metastatic potential of certain cancer cells (26, 27) or may facilitate resistance to chemical induction of apoptosis (28).

Using Q-PCR, we showed that the microarray findings in Fig. 6 of tetrac- and tetrac NP-induced changes in abundance of specific mRNAs do reflect changes in gene expression. Q-PCR studies in Fig. 7 unequivocally document effects at 24 h on gene expression of both tetrac and tetrac NP for all seven genetic targets, confirming both drug-induced inhibition (*VEGFA*; *CTNNA1*) and activation (*THBS1*; *CASP2*; *DFFA*; *FAF1*; *CASP8AP2*) of mRNA expression for corresponding genes.

Discussion

Medullary carcinoma of the human thyroid gland is a tumor that responds unsatisfactorily to conventional che-

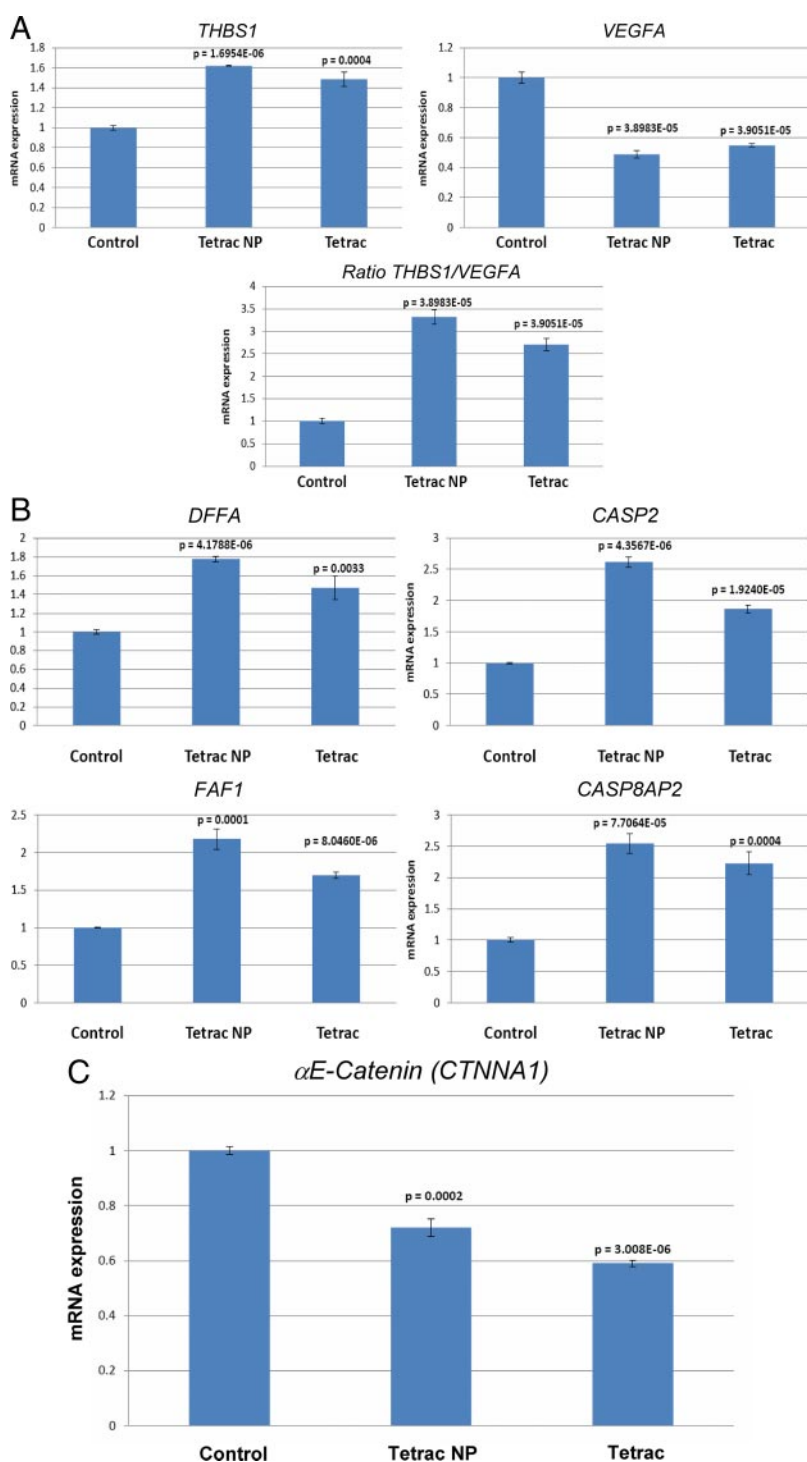


FIG. 7. Results of the Q-PCR analysis of mRNA expression in h-MTC cells treated *in vitro* with tetrac or tetrac NP. A, Average values from triplicate analyses of mRNAs of the angiogenesis-relevant *VEGFA* and *THBS1* (*thrombospondin 1*) genes in control and treated tumor cells and plotting of the ratio: *VEGFA/THBS1*. B, Average values from triplicate analyses of mRNAs of the apoptosis-relevant *CASP2*, *DFFA*, *FAF1*, and *CASP8AP2* genes in control and treated tumor cells. C, Average values from triplicate analyses of mRNA of the α E-catenin (*CTNNA1*) gene in control and treated h-MTC cells.

motherapy (13) and to radiation (29). We show here that unmodified tetrac and tetrac NP are effective inhibitors of growth of human medullary carcinoma xenograft in the nude mouse. Administered parenterally, the agents promptly

decreased tumor volume and over the course of 3 wk of treatment reduced tumor size below that of the initial volume of implanted cells. Tetrac is a deaminated analog of T_4 that inhibits the binding of agonist thyroid hormone analogs, T_4 and T_3 , to the plasma membrane receptor for iodothyronines that has been described on integrin $\alpha\beta 3$ (1). Acting at its cell surface receptor, thyroid hormone has been shown to be a proliferative factor for a variety of tumor cells (4, 5, 30) and to be proangiogenic (1–3, 31, 32). Tetrac blocks these effects (1–3). The pituitary-thyroid axis is intact in the nude mouse (33), and it is assumed that endogenous thyroid hormone is one of the host factors that permit the growth of tumor xenografts, such as those of medullary carcinoma of the thyroid in the present report. In our studies, tetrac NP was 10 times more effective than unmodified tetrac as an antiproliferative agent. The nanoparticle does not gain access to the cell interior, and thus the tetrac ether-bonded to the PLGA particle via the outer ring hydroxyl can act only at the integrin receptor—where it is exclusively an antagonist—and not at the nuclear receptor for thyroid hormone. Unmodified tetrac does gain access to the cell and can interact with thyroid hormone, where it is a low potency agonist (thyromimetic) (6). The increased potency of tetrac NP (*vs.* unmodified tetrac) as an antiproliferative agent may reflect 1) the presentation of the ligand (tetrac) to the receptor site when it is attached to the nanoparticle; or 2) action(s) of unmodified tetrac inside the cell that support cell proliferation, combined with antiproliferative effects of tetrac at the integrin.

The present studies also reveal that the antiangiogenic activity of tetrac that has been shown in the chick CAM model (2) and the microvascular endothelial cell-Matrigel assay (32) is also apparent in the xenograft-bearing intact nude mouse. Both unmodified tetrac and tetrac NP reduced the vascularity of medullary carcinoma tumors in our studies. Antiangiogenic agents clinically directed at a specific vascular growth factor have come to be regarded as adjuncts to standard chemotherapy, rather than as primary anticancer modalities (34). We might

therefore conclude that the effect of tetrac on medullary carcinoma of the thyroid secondarily involves antiangiogenesis. On the other hand, tetrac blocks the effects of more than one vascular growth factor, *e.g.* VEGF and bFGF, and thus antiangiogenesis in the present studies of tetrac may be more important than the adjunctive effect obtained clinically with agents that target a single vascular growth factor or vascular growth factor receptor.

Microarray and Q-PCR studies included here provide additional insight into the antiangiogenic activity of tetrac. The latter, either unmodified or as a nanoparticle, was shown to down-regulate the proangiogenic *VEGFA* gene and to induce significantly the expression of *thrombospondin* (*THSP1*), whose gene product is an endogenous antiangiogenic protein. *THSP1* is usually suppressed in tumor cells (35).

The action of tetrac on medullary carcinoma tumor volume had two components: a relatively acute effect that was apparent within 1–3 d of the initiation of tetrac treatment (Figs. 2 and 3) and a progressive effect. The relatively acute effects of tetrac formulations on xenograft volume shown here are thought by us to be due to the antiangiogenic activity of tetrac (7), which includes not only inhibition of the proangiogenic action of endogenous agonist thyroid hormone (1, 2) but also antagonism of the activities of VEGF and bFGF (7). Certainly, the vasculature of the xenografts was substantially reduced by tetrac and tetrac NP (Fig. 5). The progressive decrease in tumor volume that occurred over 3 wk of tetrac treatment we ascribe to the proapoptotic activity of tetrac (12). Consistent with this explanation, results of mRNA studies (Figs. 6 and 7) revealed significant, coherent effects of tetrac NP on several apoptosis-relevant genes, including *DFFA* (36), *FAF1* (37), and *CASP8AP2* (38). *CASP2* was also up-regulated by treatment; the gene product may relate to apoptosis or to tumor suppression (24). The mechanisms of action of tetrac in the tumor cell setting thus include: 1) inhibition at the integrin receptor for thyroid hormone of the proliferative effects of circulating thyroid hormones (4, 5, 12); and 2) support of apoptosis.

We would also point out that targeting an integrin with tetrac may induce loss of cell anchorage and the form of apoptosis termed anoikis (39) or separation of cells from the tumor mass into the circulation. Finally, tetrac in the xenograft setting may induce necrosis in the grafted cells that was not seen in *in vitro* studies of the action of this thyroid hormone antagonist.

The present experiments were not designed to assess toxicology of systemically administered unmodified tetrac and tetrac NP. However, at the dosage used in these mouse xenograft studies, there was no mortality in the control animals or in those that were treated with formulations

of tetrac for 3 wk. Weight gain in the treated and untreated animals was identical, indicating no specific adverse effect of tetrac or tetrac NP on appetite or metabolism. An effect on the latter was a possibility in the case of unmodified tetrac because of the access of this agent to the cell interior and the possibility of induction of low-grade hyperthyroidism.

The comparison here of tetrac and tetrac NP is useful in several contexts. First, the nanoparticulate is effective in reducing tumor volume and tumor vascularity. Second, tetrac NP has increased potency, compared with unmodified tetrac, that permits the use of lower dosing of the active agent–tetrac–covalently bound to PLGA. Third, if longer term therapy with unmodified tetrac reveals a hypermetabolic effect of the agent, this undesirable action is likely to be due to cellular uptake of unmodified tetrac, a low-grade thyromimetic, and will be avoided by use of the nanoparticle.

We have shown elsewhere that tetrac NP is an effective anticancer agent when administered on alternate days (40), rather than daily as in the current studies. Tetrac NP is also antiproliferative in xenograft models when administered at 3-d intervals (Yalcin, M., S. A. Mousa, D. J. Bharali, and P. J. Davis, unpublished observations), but longer dosing intervals have not yet been tested. Withdrawal of tetrac NP permits some regrowth of certain xenografts (40), but reinstatement of the agent reduces tumor volume (Yalcin, M., S. A. Mousa, and D. J. Bharali, unpublished observations). These findings support some optimism that these formulations of tetrac may have clinical applications.

Acknowledgments

Address all correspondence and requests for reprints to: Paul J. Davis, M.D., Ordway Research Institute, 150 New Scotland Avenue, Albany, New York 12208. E-mail: pdavis@ordwayresearch.org.

This work was supported by the Charitable Leadership Foundation/Medical Technology Acceleration Program, by the Pharmaceutical Research Institute of Albany College of Pharmacy, and by an endowment established at Ordway Research Institute by M. Frank Rudy and Margaret C. Rudy.

Disclosure Summary: The authors have nothing to disclose.

References

- Bergh JJ, Lin HY, Lansing L, Mohamed SN, Davis FB, Mousa S, Davis PJ 2005 Integrin $\alpha\beta3$ contains a cell surface receptor site for thyroid hormone that is linked to activation of mitogen-activated protein kinase and induction of angiogenesis. *Endocrinology* 146: 2864–2871
- Davis FB, Mousa SA, O'Connor L, Mohamed S, Lin HY, Cao HJ, Davis PJ 2004 Proangiogenic action of thyroid hormone is fibroblast

- growth factor-dependent and is initiated at the cell surface. *Circ Res* 94:1500–1506
3. Mousa SA, O'Connor L, Davis FB, Davis PJ 2006 Proangiogenesis action of the thyroid hormone analog 3, 5-diiodothyropropionic acid (DITPA) is initiated at the cell surface and is integrin-mediated. *Endocrinology* 147:1602–1607
 4. Davis FB, Tang HY, Shih A, Keating T, Lansing L, Hercbergs A, Fenstermaker RA, Mousa A, Mousa SA, Davis PJ, Lin HY 2006 Acting via a cell surface receptor, thyroid hormone is a growth factor for glioma cells. *Cancer Res* 66:7270–7275
 5. Lin HY, Tang HY, Shih A, Keating T, Cao G, Davis PJ, Davis FB 2007 Thyroid hormone is a MAPK-dependent growth factor for thyroid cancer cells and is anti-apoptotic. *Steroids* 72:180–187
 6. Moreno M, de Lange P, Lombardi A, Silvestri E, Lanni A, Goglia F 2008 Metabolic effects of thyroid hormone derivatives. *Thyroid* 18:239–253
 7. Mousa SA, Bergh JJ, Dier E, Rebbaa A, O'Connor LJ, Yalcin M, Aljada A, Dyskin E, Davis FB, Lin HY, Davis PJ 2008 Tetraiodothyroacetic acid, a small molecule integrin ligand, blocks angiogenesis induced by vascular endothelial growth factor and basic fibroblast growth factor. *Angiogenesis* 11:183–190
 8. Cody V, Davis PJ, Davis FB 2007 Molecular modeling of the thyroid hormone interactions with $\alpha\beta3$ integrin. *Steroids* 72:165–170
 9. Plow EF, Haas TA, Zhang L, Loftus J, Smith JW 2000 Ligand binding to integrins. *J Biol Chem* 275:21785–21788
 10. Masson-Gadais B, Houle F, Laferrière J, Huot J 2003 Integrin $\alpha\beta3$ requirement for VEGFR2-mediated activation of SAPK2/p38 and Hsp90-dependent phosphorylation of focal adhesion kinase in endothelial cells activated by VEGF. *Cell Stress Chaperones* 8:37–52
 11. Sahni A, Francis CW 2004 Stimulation of endothelial cell proliferation by FGF-2 in the presence of fibrinogen requires $\alpha\beta3$. *Blood* 104:3635–3641
 12. Rebbaa A, Chu F, Davis FB, Davis PJ, Mousa SA 2008 Novel function of the thyroid hormone analog tetraiodothyroacetic acid: a cancer chemosensitizing and anti-cancer agent. *Angiogenesis* 11:269–276
 13. Schlumberger M, Carlomagno F, Baudin E, Bidart JM, Santoro M 2008 New therapeutic approaches to treat medullary thyroid carcinoma. *Nat Clin Pract Endocrinol Metab* 4:22–32
 14. Raue F, Frank-Raue K 2007 Multiple endocrine neoplasia type 2: 2007 update. *Horm Res* 68 (Suppl 5):101–104
 15. Jeffery H, Davis SS, O'Hagan DT 1991 The preparation and characterization of poly(lactide-co-glycolide) microparticles. 1. Oil-in-water emulsion solvent evaporation. *Int J Pharm* 77:169–175
 16. Song C, Labhasetwar V, Cui X, Underwood T, Levy RJ 1998 Arterial uptake of biodegradable nanoparticles for intravascular local drug delivery: results with an acute dog model. *J Control Release* 54:201–211
 17. Hermanson GT 1996 Bioconjugate technique. San Diego: Academic Press; 617–618
 18. Bergström K, Holmberg K, Safranjan A, Hoffman AS, Edgell MJ, Kozłowski A, Hovanec BA, Harris JM 1992 Reduction of fibrinogen adsorption on PEG-coated polystyrene surfaces. *J Biomed Mater Res* 26:779–790
 19. Mousa S, Mousa SA 2006 Cellular and molecular mechanisms of nicotine's proangiogenesis activity and its potential impact on cancer. *J Cell Biochem* 97:1370–1378
 20. Glinsky GV, Berezovska O, Glinskii AB 2005 Microarray analysis identifies a death-from-cancer signature predicting therapy failure in patients with multiple types of cancer. *J Clin Invest* 115:1503–1521
 21. Glinsky GV, Higashiyama T, Glinskii AB 2004 Classification of human breast cancer using gene expression profiling as a component of the survival predictor algorithm. *Clin Cancer Res* 10:2272–2283
 22. Glinsky GV, Glinskii AB, Stephenson AJ, Hoffman RM, Gerald WL 2004 Gene expression profiling predicts clinical outcome of prostate cancer. *J Clin Invest* 113:913–923
 23. Glinsky GV, Kronen-Herzig A, Glinskii AB, Gebauer G 2003 Microarray analysis of xenograft-derived cancer cell lines representing multiple experimental models of human prostate cancer. *Mol Carcinog* 37:209–221
 24. Kitevska T, Spencer DM, Hawkins CJ 2009 Caspase-2: controversial killer or check-point controller? *Apoptosis* 14:829–848
 25. Lin HY, Tang HY, Keating T, Wu YH, Shih A, Hammond D, Sun M, Hercbergs A, Davis FB, Davis PJ 2008 Resveratrol is pro-apoptotic and thyroid hormone is anti-apoptotic in glioma cells: both actions are integrin- and thyroid hormone-mediated. *Carcinogenesis* 29:62–69
 26. Davidson B, Berner A, Nesland JM, Risberg B, Berner HS, Tropè CG, Kristensen GB, Bryne M, Ann Florenes V 2000 E-Cadherin and α -, β - and γ -catenin protein expression is upregulated in ovarian carcinoma cells in serous effusions. *J Pathol* 192:460–469
 27. Imai T, Horiuchi A, Shiozawa T, Osada R, Kikuchi N, Ohira S, Oka K, Konishi I 2004 Elevated expression of E-cadherin and α , β and γ catenins in metastatic lesions compared with primary epithelial ovarian carcinomas. *Hum Pathol* 35:1469–1476
 28. Matsubara S, Ozawa M 2001 Expression of α -catenin in α -catenin-deficient cells increases resistance to sphingosine-induced apoptosis. *J Cell Biol* 154:573–584
 29. Hoff AO, Hoff PM 2007 Medullary thyroid carcinoma. *Hematol Oncol Clin North Am* 21:475–488; viii
 30. Tang HY, Lin HY, Zhang S, Davis FB, Davis PJ 2004 Thyroid hormone causes mitogen-activated protein kinase-dependent phosphorylation of the nuclear estrogen receptor. *Endocrinology* 145:3265–3272
 31. Mousa SA, O'Connor LJ, Bergh JJ, Davis FB, Scanlan TS, Davis PJ 2005 The proangiogenic action of thyroid hormone analogue GC-1 is initiated at an integrin. *J Cardiovasc Pharmacol* 46:356–360
 32. Mousa SA, Davis FB, Mohamed S, Davis PJ, Feng X 2006 Proangiogenesis action of thyroid hormone and analogs in a three-dimensional in vitro microvascular endothelial sprouting model. *Int Angiol* 25:407–413
 33. Theodossiou C, Skrepnik N, Robert EG, Prasad C, Axelrad TW, Schapira DV, Hunt JD 1999 Propylthiouracil-induced hypothyroidism reduces xenograft tumor growth in athymic nude mice. *Cancer* 86:1596–1601
 34. Bergers G, Hanahan D 2008 Modes of resistance to anti-angiogenic therapy. *Nat Rev Cancer* 8:592–603
 35. Almog N, Ma L, Raychowdhury R, Schwager C, Erber R, Short S, Hlatky L, Vajkoczy P, Huber PE, Folkman J, Abdollahi A 2009 Transcriptional switch of dormant tumor to fast-growing angiogenic phenotype. *Cancer Res* 69:836–844
 36. Nordström EA, Rydén M, Backlund EC, Dahlman I, Kaaman M, Blomqvist L, Cannon B, Nedergaard J, Arner P 2005 A human-specific role of cell death-inducing DFFA (DNA fragmentation factor- α)-like effector A (CIDEA) in adipocyte lipolysis and obesity. *Diabetes* 54:1726–1734
 37. Manges CW, Altomare DA, Testa JR 2009 FAS-associated factor 1 (FAF1): diverse functions and implications for oncogenesis. *Cell Cycle* 8:2528–2534
 38. Flotho C, Coustan-Smith E, Pei D, Iwamoto S, Song G, Cheng C, Pui CH, Downing JR, Campana D 2006 Genes contributing to minimal residual disease in childhood acute lymphoblastic leukemia: prognostic significance of CASP8AP2. *Blood* 108:1050–1057
 39. Chiarugi P, Giannoni E 2008 Anoikis: a necessary death program for anchorage-dependent cells. *Biochem Pharmacol* 76:1352–1364
 40. Yalcin M, Bharali DJ, Dyskin E, Dier E, Lansking L, Mousa SS, Davis FB, Davis PJ, Mousa SA 2009 Tetraiodothyroacetic acid (tetrac) tetrac nanoparticles effectively inhibit growth of human follicular thyroid cell carcinoma. *Thyroid*